 DOI 10.1515/secm-2014-0069 — Sci Eng Compos Mater 2015; 22(5): 555–564

Zhiyuan Zhang, Yuqiu Yang* and Hiroyuki Hamada

The effects of open holes on the fracture behaviors and mechanical properties of glass fiber mat composites

Abstract: In this paper, composite specimens were fabricated from a glass fiber chopped strand mat and unsaturated polyester resin using the hand lay-up method. To evaluate the effects of open holes on the mechanical properties, different factors, including the volume fraction of glass fiber and material thickness were investigated. Both the unnotched strength of smooth specimens and the notched strength of specimens with holes, increased as volume fraction increased, but the trends were different. For notched specimens with closer volume fractions, increased thickness or width-to-depth ratio led to a lower resistance on the open hole. In investigating the fracture behaviors of notched specimens, two different fracture areas were distinguished: parallel areas and fan-shaped areas. The length of each parallel area was measured. To evaluate the material properties, characteristic distance was calculated using linear elastic methods in finite element software (MSC-Marc, MSC Software Corporation, Tokyo, Japan). The results revealed that characteristic distance has a good correspondence with parallel area length.

Keywords: characteristic distance; finite element; glass fiber chopped mat; notched strength.

***Corresponding author: Yuqiu Yang,** Donghua University, Songjiang District, Shanghai 201620, P.R. China, e-mail: amy_yuqiu_yang@dhu.edu.cn
Zhiyuan Zhang and Hiroyuki Hamada: Kyoto Institute of Technology, Matsugasaki, Sakyo-ku, Kyoto 606-8585, Japan

1 Introduction

Due to its versatile properties, fiber reinforced plastic (FRP) has been used in various industries for many decades, including aircraft, automobiles, ship building, and housing products [1–6]. However, because of its complex failure modes, anisotropic properties, and the relative newness of the material compared with metals, design rules, and empirical data are insufficient for designing FRP structures. As a result, structures are usually hybrids made of composites and metals instead of composite structures, including large vessels, automotive drive shafts, and robotic structures [7]. One crucial limitation is joint weakness. During use, joints are usually needed to connect the different parts of the structure. Joints can be divided into three types: joints bonded with adhesive; mechanically fastened joints, which use pins or bolts; and combination joints [8, 9]. Bonded joints have low weight and a good seal to the structure, but need certain conditions for the bonded surfaces, and can have some negative effects on the environment. Comparatively, mechanically fastened joints require no preparation of the target surfaces, reducing complexity.

It is reported that mechanical joints are very convenient and universally used in the assembly of structural components, due to their ability to transmit high loads, good resistance to interlaminar stresses, and suitability for almost any environmental conditions [10]. The basic method to make mechanical joints is to drill holes in two parts, which are then joined by inserting a mechanical bolt through the hole to affix the fasteners. However, as stress concentrates near the hole, these joints can fail more easily [11–16]. Unlike metallic materials, stress transmission is more complicated in composite materials due to their different components, which cause more complicated fracture characteristics and are difficult to predict. More research needs to be done to provide theoretical support for design and further application.

The notched strength of composite materials is an important property that has gained extensive use by designers. Many researchers have devoted themselves to investigating the effects of different factors on notched strength, including laminate size and thickness, notch size, ply orientation and thickness, machining quality, and material constituents. All of these factors affect the final properties by changing the damage growth process, and interact with each other to enhance the individual effects. Green et al. conducted an extensive experimental investigation into the effects of scaling notched composites [17]. They developed a quasi-isotropic laminate with a stacking sequence of $(45_m/90_m/\text{-}45_m/0_m)_{ns}$. Increasing the subscripts m and n allow increased ply-level scaling and

sublaminate-level scaling composites, respectively. They distinguished three kinds of fracture, including brittle, where fiber failure occurs throughout the thickness of the laminate; pull-out, where some or all of the off-axis plies fail via delamination and matrix cracking; and delamination, where complete gauge delamination occurs in section -45/0. Different fracture behavior was used to explain the relationship between notched strength and size. It was found that, in specimens with holes of identical diameter, notched strength decreased as specimen thickness increased. The thicker specimens were considered more likely to generate delamination because thicker specimens could provide greater energy. The effects of scale on composite materials with open holes were also investigated by Orifici and Herszberg [18]. Different length scales were employed in the test, including change of ply thickness through the use of single-ply and 4-ply laminates, and changes in specimen geometry through scaling the in-plane dimensions with hole diameter. It was found that the failure mode changed when thickness was increased. Matrix cracking first occurred at the edge of the open hole, which then led to delamination between plies in thicker specimens. This kind of damage was more related to the ply thickness compared to in-plane dimensions. However, most of the research was focused on continuous fiber. Only limited research has been found on chopped fiber composites.

Fiber configuration is also an important factor affecting the properties of notched laminated composite. Lindhagen and Berglund investigated notch sensitivity and damage mechanisms of glass mat reinforced polypropylene [19]. They used a short fiber mat and a swirled fiber mat to fabricate a composite under close volume fraction of glass fibers. Specimens of identical dimensions were drilled using three types of drill (HAM Japan Co., Ltd., Tokyo, Japan), with diameters of 5 mm, 10 mm, and 15 mm. The short fiber material was found to have higher unnotched strength, but similar notched strength to the swirled fiber material, which indicates higher notch sensitivity in the short fiber mat composite compared to the swirled mat composite. By conducting a tensile test 10 degrees off-axis (fiber direction) on specimens with open holes, Mendoza et al. [20] investigated the effects of the uncertainty of the fiber volume fraction in the failure location and the magnitude of the strain at failure. A Bayesian updating probability distribution was used to assess confidence in the model prediction, combined with both experimental and simulation data. In the specimens used, it was found that the probabilistic distribution of the failure initiation location was caused partly by the dispersion in the fiber volume fraction. In Bayesian analysis, the confidence factors of the model supported by the experimental data were over 0.80. These studies revealed the influence of fiber configuration and volume fraction on notched property. However, more accurate results are needed to evaluate and predict the properties of composite materials.

Moreover, many researchers investigated the stress and fracture behavior of laminar composite with circular holes, due to the inherent relation with notched properties. O'Higgins and McCarthy compared damage progression and fracture behavior in carbon fiber reinforced plastic (CFRP), and glass fiber reinforced plastic (GFRP) to investigate tensile testing with open-hole composites [21]. Different fiber configurations were compared, including one quasi-isotropic ($[45/0\text{-}45/90]_{2s}$), and three cross-ply ($[90/0]_{4s}$, $[90/0]_{2s}$, $[90_2/0_2]_s$). It was concluded that the damage and failure behaviors were very similar. For the quasi-isotropic configuration, the initial crack occurred in the matrix of ±45° and 90° plies, and delamination happened before failure. For the cross-ply configuration, the matrix crack happened in the 90° plies at beginning, and then a pair of triangular damage areas appeared around the hole and extended until failure.

In order to analyze and describe the characteristics of stress to a circular hole, Whitney and Nuismer introduced the concept of characteristic distance [22]. Characteristic distance is used to derive point-stress and average-stress failure criteria, and is widely used in predicting the notched strength of open-hole composite. In point-stress failure criteria, the characteristic distance (d_0) is the length from the hole edge to the point where the stress equals the unnotched strength, when the notched material carries maximum load. For average-stress failure criteria, the characteristic distance (a_0) is the length from the edge of the hole to the point where the average stress equals the unnotched strength. It was further assumed that the characteristic distance is a material property and is independent of the hole size or geometry of the plate. In order to calculate the characteristic distance, one needs to calculate the distribution of stress around the hole. For calculation, closed-form equations using two dimensional elasticity solutions are usually used. Characteristic distance can also be determined using the finite element method (FEM). Compared to closed-form solutions, FEM-based models have the advantage that the geometry and stress field near the hole may be arbitrary [23].

In this study, a glass fiber chopped strand mat (GM), and unsaturated polyester resin (UP), were used to fabricate fiber glass mat composites (GMC), with different fiber volume fractions (V_f) and laminations of 3, 5, or 7 plies. A drill with a bit 10 mm in diameter was used to drill holes for the notched specimens. The study discusses the

relationship between strength or notched strength and volume fraction. Through scanning electron microscope (SEM) observation (JEOL Ltd., Tokyo, Japan), we distinguished two fracture characteristics of notched specimens: parallel areas and fan-shaped areas. In addition, to evaluate the specimens using characteristic distance, MSC-Marc finite element analysis software was used to calculate the stress distribution around the holes of the notched specimens using the linear elastic method. The correlation between characteristic distance and the fracture characteristics of open-hole GMC is also discussed.

2 Materials and methods

2.1 Materials

A glass fiber chopped strand mat (Nitto Glasstex Co., Ltd.), with gram weight of 450 g/m^2 was used as reinforcement. The fabric was made of continuous glass fiber bundles, chopped into segments 50 mm in length. The chopped glass bundles were distributed in random directions, as shown in Figure 1.

Unsaturated polyester resin (Showa: RIGORAC 150HRBQNTNW, Showa Denko K.K. Co., Ltd., Tokyo, Japan) was used as the matrix. The resin was mixed with the hardener MEKPO (PERMEK N; NOF Corporation, Osaka, Japan) in a ratio of 100:0.7. Table 1 shows the properties of the UP as measured in lab by tensile test, with a cross-head speed of 1 mm/min.

Composites were created using three, five and seven layers of glass mat through hand lay-up molding. Composite thickness was controlled by spacers, to obtain different V_f in the range of 18%–37%, (determined by burning method according to JIS-K7052). After curing the composite at room temperature for 24 h, the specimens were heated in an oven at 100°C (for 2 h) as a post-cure.

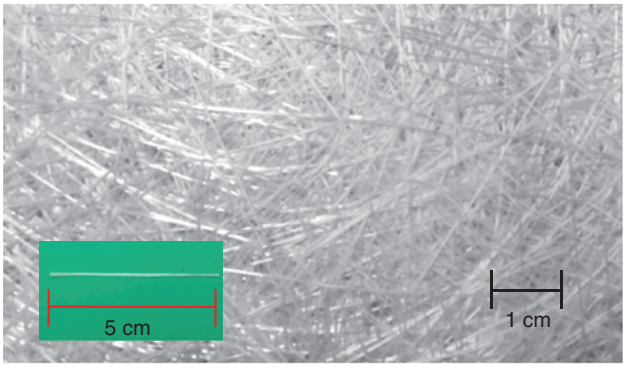

Figure 1 Glass fiber chopped strand mat.

Table 1 Properties of unsaturated polyester (UP).

Main component	Density (g/cm^3)	Modulus (GPa)	Strength (MPa)	Elongation (%)
Isophthalic acid	1.25	3.20	42.00	2.18

2.2 Specimen preparation

Firstly, smooth specimens with sizes of 20 mm×150 mm were attached to aluminum plate (25 mm in height) and tested to investigate the material constants (such as Young's modulus).

Furthermore, the notched properties of GMC were also investigated on notched specimens, where a hole was drilled into the center of the specimens. The dimensions and drilling method are illustrated in Figure 2. The wood under the specimens was used to protect the materials from delamination during the drilling process.

In order to avoid the effects of micro-damage around the hole caused by the drilling process, the same 10 mm drill was used to drill all holes, with a speed of 2300 rad/min, to ensure that all the notched specimens had holes in similar conditions. Different widths, including 20 mm, 30 mm, and 50 mm, were cut to obtain different width-to-diameter (w/d) ratios, specifically 2, 3, and 5. For the specimens with w/d ratios of 2 or 3, the total length is 150 mm, and the tabs extend 25 mm on both sides, while, for w/d=5 specimens, the length and the tabs are 250 mm and 50 mm, respectively.

2.3 Tensile test

Tensile testing was performed using an Instron universal testing machine (Instron Japan Co., Ltd., Kawasaki, Japan), at a speed of 1 mm/min. Additionally, a strain gauge (Kyowa KFG-10-120-C1-11, Kyowa Electronic Instruments Co., Ltd, Tokyo, Japan) was employed to measure the strain of the smooth specimens during the testing process. For notched specimens, notched strength was calculated using formula (1). The notched strength and smooth strength were compared and analyzed with regard to V_f.

$$\sigma_N = \frac{F}{(W\text{-}D)T} \tag{1}$$

Where σ_N is notched strength, the mean strength of the notched specimens; F is maximum load; W is the width of the specimen; D is the diameter of open hole; and T is the thickness of the specimen. The coefficient of variation (C_V)

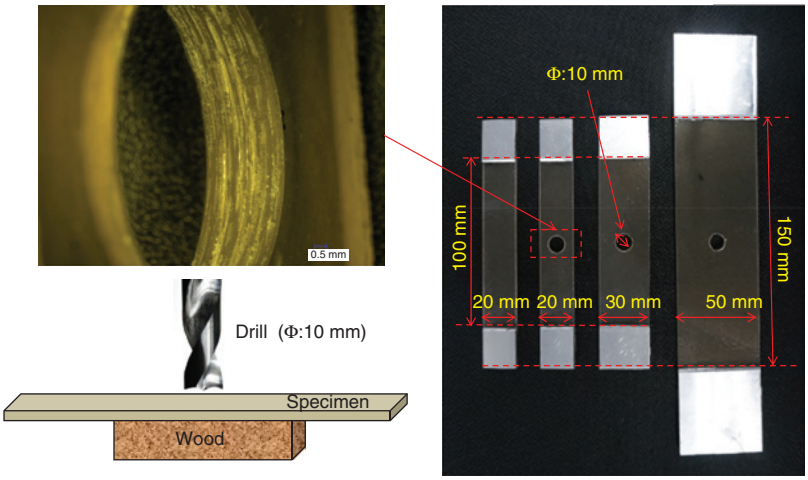

Figure 2 Dimension and preparation of specimens.

is defined as the ratio of the standard deviation σ to the mean μ. It can be calculated using formula (2):

$$C_V = \frac{\sigma}{\mu} \tag{2}$$

C_V is a normalized measure of the dispersion of a set of data. A camera system with a frame rate of 30 FPS was used to capture crack propagation during the tensile test process.

3 Results and discussion

3.1 The tensile test results of smooth specimens

The tensile modulus and strength of smooth specimens are shown in Figure 3A and B, respectively. The trend line shown was drawn according to the least square method. At the same time, the trend line equation and correlation coefficient (R) were calculated. The correlation coefficient was found by equation (3).

$$R = \frac{\sum_{i=1}^{n}(x_i - \bar{x})(y_i - \bar{y})}{\sqrt{[\sum_{i=1}^{n}(x_i - \bar{x})^2][\sum_{i=1}^{n}(y_i - \bar{y})^2]}} \tag{3}$$

The correlation coefficient gives the degree to which a line generated by the least square method fits the original data. If x and y have a strong linear correlation, R^2 is close to 1. The results show that both the Young's modulus and strength were increased with the V_f of glass fiber.

3.2 The tensile test results of notched specimens

Notched strength is shown in Figure 4. Each size of notched specimen is represented with a different shape,

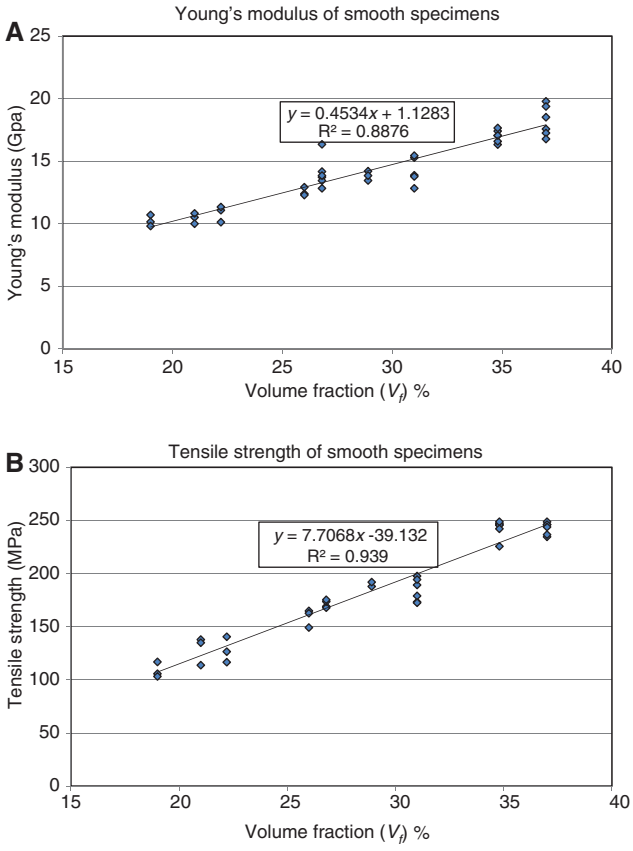

Figure 3 Tensile test result of smooth specimens.

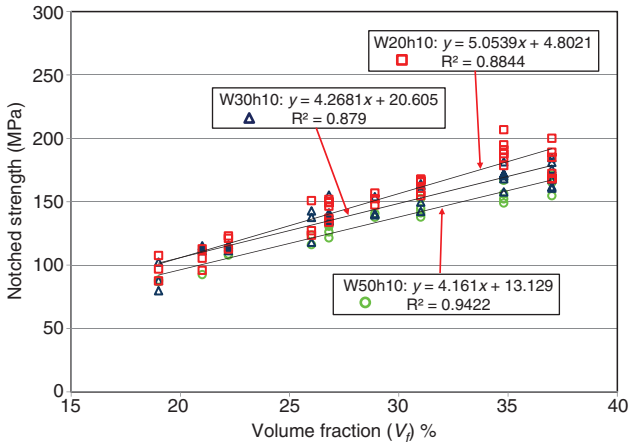

Figure 4 Tensile test result of notched specimens.

based on width. From the trend line described, we can observe that notched strength decreases with the increase of the width-to-diameter ratio. According to the slope of the trend line equation, specimens with lower w/d ratio gain notched strength more easily when V_f is increased.

The comparison between smooth strength and notched strength for the specimens with closed V_f but different laminated plies is shown in Figure 5, included 3, 5, and 7-ply specimens with a V_f of 31%, 31%, and 29% respectively. For example, GM3 represents specimens with three layers of glass mat. The decreasing ratio of notched strength from smooth strength of each specimen is shown here. We observed that specimens with a higher w/d ratio had lower notched strength when compared to specimens with the same number of layers. For example, in 3-ply specimens, the decreasing ratios were 10%, 13%, and 21% for specimens with w/d ratios of 2, 3, and 5, respectively. The results also illustrate that notched strength decreased more obviously in 7-ply specimens, which have greater thickness. Consider that the decreasing ratios were 20%, 24%, and 27%, all the largest decreases in percentage. This phenomenon suggests that thickness has a strong effect on the sensitivity of specimens with holes. Our data suggests that GMC with higher thickness was more sensitive to an open hole.

3.3 Damage process of notched specimens

A 30-mm wide specimen was selected to explain the damage process of notched specimens shown in Figure 6. The first picture illustrates the specimen during the initial tensile process. The second and third pictures are of specimens carrying maximum load and just after, respectively. The specimen in the fourth picture is totally broken. As the applied load increased, some sound could be heard, expected to be the resin fracturing and the fiber debonding from the matrix. As the test process advanced, the fracture sounds became louder and more frequent, and significant cracks appeared at the edge of the hole, slowly extending outward. Damage near the hole became opaque, as seen in the second and third pictures. After reaching the state shown in the third picture, the specimens would be destroyed suddenly and very fast (within 0.03 s).

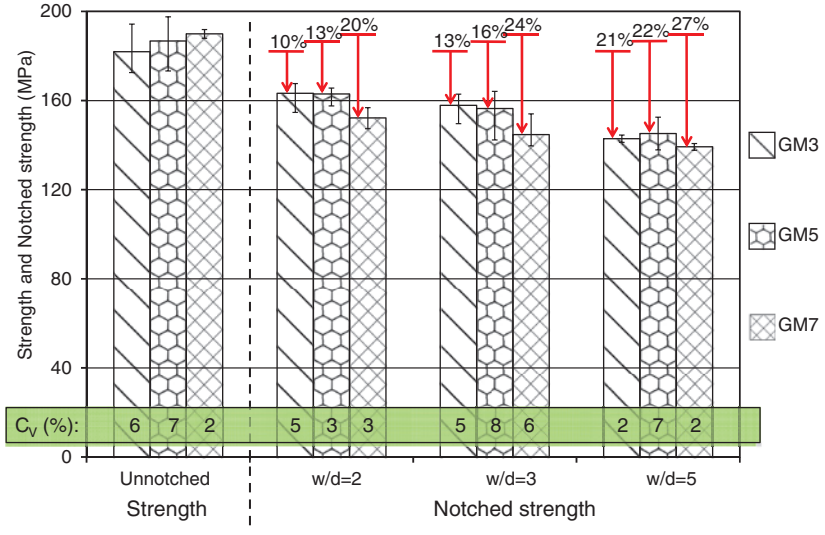

Figure 5 Notched strength decreasing of different specimens in dimension.

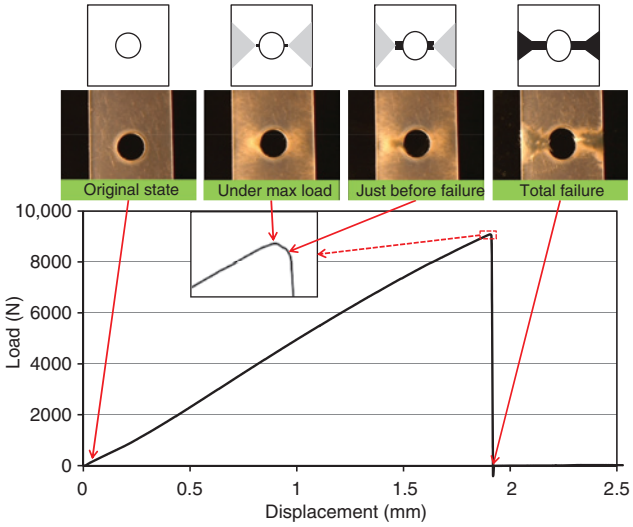

Figure 6 Fracture process of notched specimen.

3.4 Fracture characteristics of notched specimens

After the tensile test, the fracture section was not trimmed. The typical fracture zone could be divided into two parts, as shown in Figure 7. This typical fracture formation is closely related to the different stages of the tensile testing process.

During tensile testing, the cracks occurring at the edge of hole and extending to the outside at the first stage make up the parallel area, due to its relatively stable height. After the parallel area forms, the size of the damaged area increases rapidly in the second stage. After the second stage, the damaged area shows a fan-shaped distribution.

To investigate the parallel length relative to the peak load, the length of the parallel area was measured. Each specimen has two values of parallel area length, one for each side. Some results are displayed in Figure 8 as examples. Length was found to increase with the width-to-diameter ratio.

3.5 SEM observation on the fracture surface of notched specimens

The sketch of the different fractures in the notched specimens and the SEM observation results are shown in Figure 9. In the parallel area, most of the fiber was broken near the surface, caused by concentrated stress at the edge of the hole. As the fracture extended to the outside, the stress was distributed, and the width of the fracture area increased. During this period, the stress was not sufficiently concentrated to break the fibers. The cracks developed in a different direction, changing from

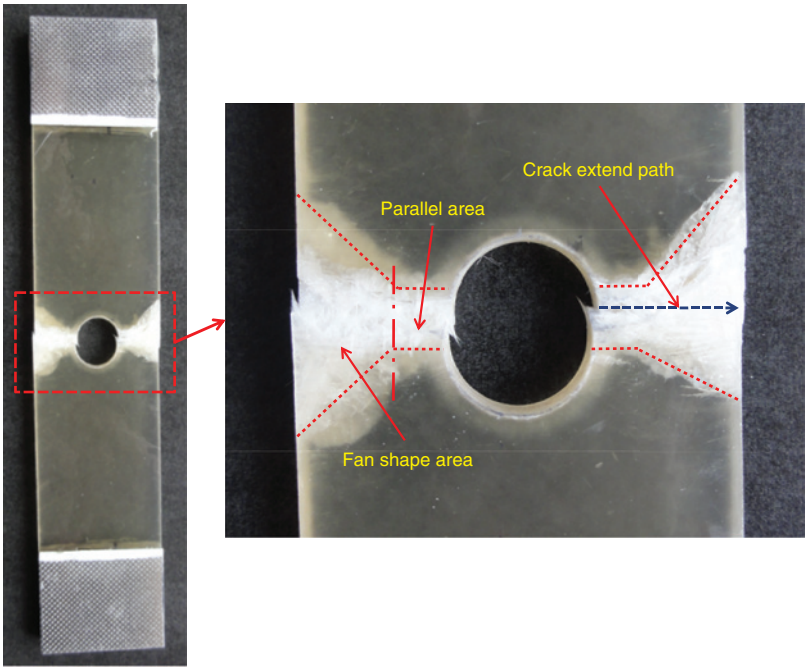

Figure 7 Fracture characteristics of notched specimen which were determined as parallel and fan shape areas.

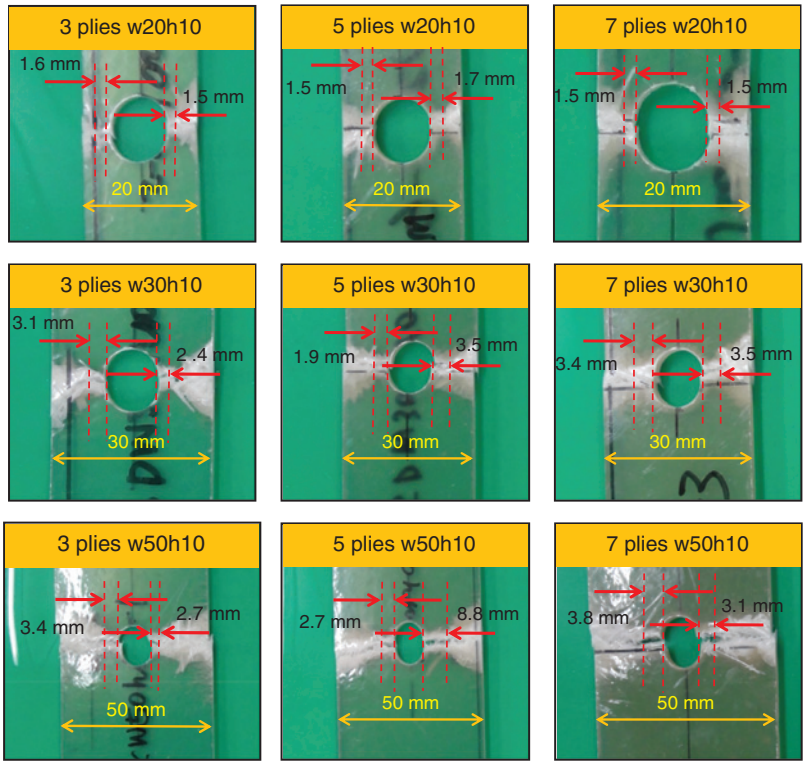

Figure 8 Measurement of parallel area length.

perpendicular to the specimen plane to parallel to the specimen plane, which caused pulling out or shear fractures in the glass fiber. To confirm these fracture characteristics, more notched specimens were observed. The typical observations are shown in Figure 10 through different magnifications.

3.6 Characteristic distance

When notched specimens carried maximum load, there were two points on the line through the center of the hole perpendicular to the loading direction. At these points, the stress was equal to the strength of

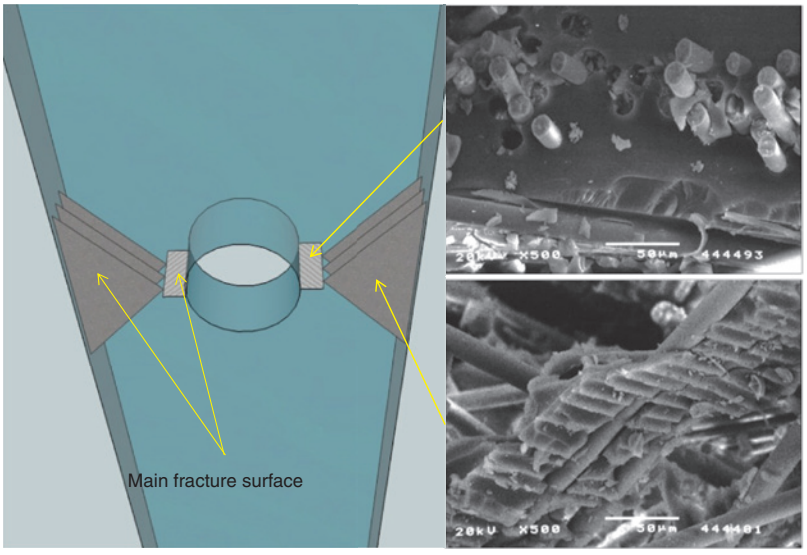

Figure 9 Fracture characteristics of notched specimen in parallel area and fan shape area.

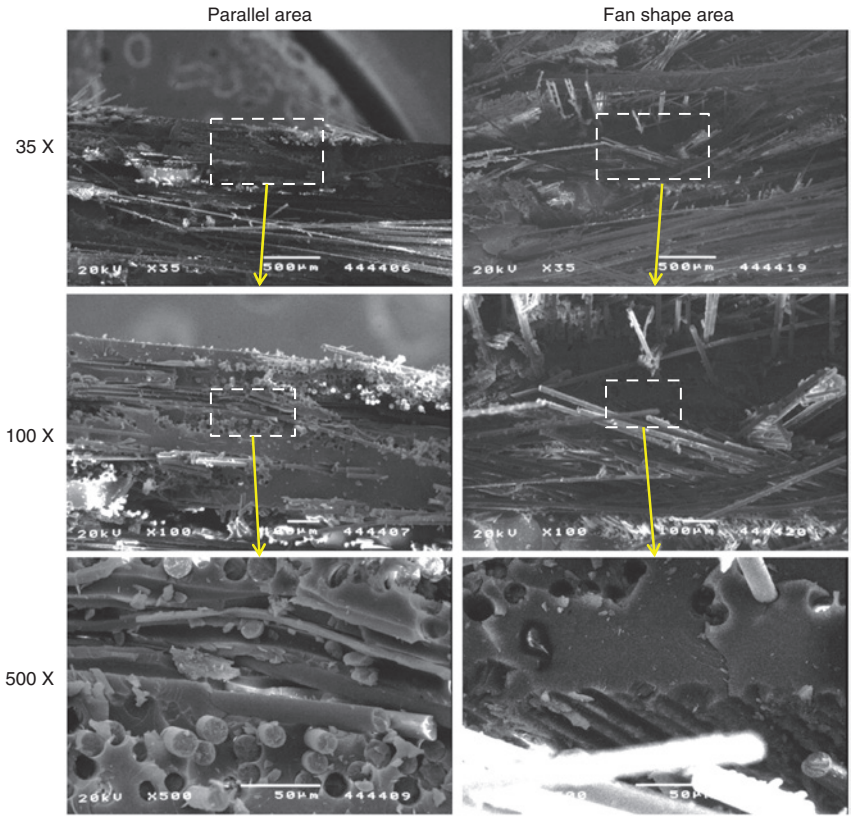

Figure 10 Fracture of notched specimen in parallel area (fiber fractures) and fan shape area (pulling out or shearing fracture of glass fibers).

the unnotched material. The minimum distance from the edge of the hole to this point was defined as characteristic distance, according to point stress criterion theory [22].

In this study, the characteristic distance was calculated by finite element analysis (MSC-Marc), for further understanding of the fracture behaviors of open-hole glass mat composite. In the simulation, a triangle element of three points (element type 6), was used. To obtain more accurate results around the hole, the element near the hole was meshed more closely with the specimen. As the chopped glass fiber of the composite was non-woven and randomly distributed, the interlaminar and intralaminar properties were assumed to be identical. The Young's modulus and Poisson's ratio were obtained from smooth specimens for each V_f and used in the simulation. The maximum load of the notched specimen was also applied here. The tensile process for notched specimens was treated as an isotropic linear elastic plane strain problem. The maximum load and stress distribution around the open hole under unit displacement were calculated using the simulation. At that point, the actual stress distribution was calculated according to the ratio of calculated maximum load to the experimental maximum load, according to linear elastic mechanics. The results for all notched specimens are listed in Table 2. From the results, we found that the characteristic distance increased with the width-to-diameter ratio, which supports the experimental results, i.e., the characteristic distance is related to specimen dimensions [24].

3.7 Correlation between parallel area length and characteristic distance

Comparing parallel area length and characteristic distance shows that the parallel area length of most notched specimens was rather close to the characteristic distance, as all of the results illustrate in Figure 11.

Each notched specimen has two values of parallel area length, with value 1 representing the larger length, and 2 the shorter length. Most of the points are close to the line, especially those specimens with low width-to-diameter ratio. According to the relationship between characteristic distance and notch sensitivity, increasing the parallel area

Table 2 Calculation results of characteristic distance (d_0).

				3 Plies					5 Plies					7 Plies
No.	Volume fraction (%)	w/d	Thickness (mm)	Characteristic distance (mm)	No.	Volume fraction (%)	w/d	Thickness (mm)	Characteristic distance (mm)	No.	Volume fraction (%)	w/d	Thickness (mm)	Characteristic distance (mm)
1	18.8	2	2.3	2.0	1	20.8	2	3.8	1.9	1	22.2	2	5.5	2.0
2		2	2.3	2.2	2		2	3.8	1.9	2		2	5.5	2.0
3		2	2.3	1.5	3		2	3.8	1.5	3		2	5.5	1.9
4		3	2.4	2.3	4		3	3.8	2.9	4		3	5.5	2.5
5		3	2.4	3.0	5		3	3.8	2.4	5		3	5.5	2.8
6		3	2.4	1.7	6		3	3.7	2.9	6		3	5.4	2.9
7		5	2.3	3.0	7		5	3.8	1.9	7		5	5.4	3.2
8		5	2.4	2.8	8		5	3.8	1.9	8		5	5.5	3.1
9	26.3	2	2.0	1.5	9	26.8	2	3.3	1.5	9	26.8	2	4.4	1.5
10		2	2.0	1.5	10		2	3.3	1.8	10		2	4.4	1.5
11		2	2.0	2.0	11		2	3.3	1.5	11		2	4.4	1.5
12		3	1.9	2.9	12		3	3.3	1.7	12		3	4.4	2.3
13		3	1.9	1.7	13		3	3.3	2.3	13		3	4.4	2.2
14		3	1.9	2.4	14		3	3.3	2.3	14		3	4.3	2.9
15		5	2.0	2.0	15		5	3.3	1.9	15		5	4.4	2.5
16		5	1.9	2.5	16		5	3.3	2.3	16		5	4.4	2.5
17	31.0	2	1.8	2.0	17	31.0	2	2.8	1.9	17	28.9	2	4.1	1.5
18		2	1.8	2.0	18		2	2.8	1.5	18		2	4.1	1.5
19		2	1.8	1.5	19		2	2.8	1.8	19		2	4.1	1.5
20		3	1.7	2.3	20		3	2.8	2.8	20		3	4.1	1.7
21		3	1.7	2.9	21		3	2.8	2.6	21		3	4.1	2.3
22		3	1.7	2.9	22		3	2.8	1.7	22		3	4.1	1.7
23		5	1.7	2.5	23		5	2.8	2.4	23		5	4.1	2.4
24		5	1.7	2.7	24		5	2.8	3.1	24		5	4.1	1.9
25	37.0	2	1.5	1.1	25	34.8	2	2.5	1.5	25	34.8	2	3.3	1.1
26		2	1.5	1.5	26		2	2.4	1.9	26		2	3.3	1.1
27		2	1.5	1.1	27		2	2.4	1.5	27		2	3.3	1.5
28		3	1.5	1.3	28		3	2.5	1.7	28		3	3.4	1.3
29		3	1.6	1.3	29		3	2.4	1.3	29		3	3.2	1.3
30		3	1.6	1.3	30		3	2.5	1.7	30		3	3.2	1.3
31		5	1.5	1.4	31		5	2.4	1.9	31		5	3.5	1.4
32		5	1.5	1.9	32		5	2.4	1.4	32		5	3.6	1.4
					33	38.7	2	2.3	1.5					
					34		2	2.3	1.5					
					35		2	2.3	1.1					
					36		3	2.3	1.7					
					37		3	2.3	1.7					
					38		3	2.3	1.7					
					39		5	2.3	1.9					
					40		5	2.3	1.9					

length can enhance the resistance of GMC to the stress of an open hole.

4 Conclusion

In this study, glass fiber mat composites (Owens Corning Japan Co., Ltd., Tokyo, Japan) with different V_f and thickness were fabricated to investigate the effects of open holes on the mechanical properties. The following conclusions were obtained.

1. The fracture of GMC materials with open hole was categorized into two areas: parallel area and fan-shaped area.
2. Due to the effects of the open hole, notched strength did not increase as effectively as in smooth specimens as V_f increased. By comparing strength in specimens

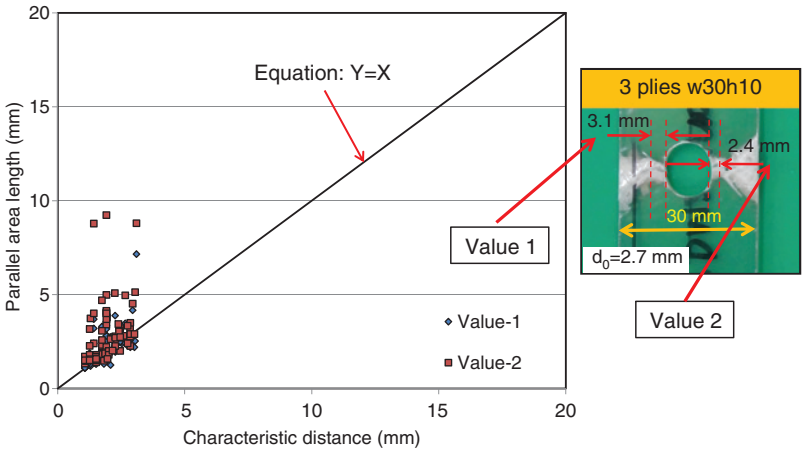

Figure 11 Correlation between characteristic distance and parallel area length.

of different thicknesses, it was found that the higher thickness or higher width-to-diameter ratio specimens had a greater decrease in the ratio of notched strength to smooth strength.

3. Characteristic distance was employed to investigate the fracture characteristics, and specimens with higher width-to-diameter ratios were found to have higher characteristic distance. This was also confirmed to have a strong correlation with parallel area length. It may be useful to predict parallel area length in the future.
4. The SEM observation of the fiber fractures indicated the difference between parallel areas and fan-shaped areas is not only on the visible, macroscopic level, but also on the microscopic level.

Received March 3, 2014; accepted April 5, 2014; previously published online June 7, 2014

References

[1] Aytac G, Onur S. *Polym. Compos.* 2010, 31, 173–178.
[2] Pakdil M. *Indian J. Eng. Mater. Sci.* 2009, 16, 79–85.
[3] Wolfrath J, Michaud V, Manson, JAE. *Polym. Compos.* 2005, 26, 361–369.
[4] Tsotsis TK, Keller S, Bardis J, Bish J. *Polym. Degrad. Stab.* 1999, 64, 207–212.
[5] Laurent D, Fabrice B, Rene G. *Mater. Sci. Forum* 2001, 404, 43–48.
[6] Kaleemulla KM, Siddeswarappa B, Satish KG. *J. Eng. Sci. Technol.* 2009, Rev. 2, 91–98.
[7] Ryosuke M, Motoko S, Akira T. *Composites, Part A.* 2008, 39, 154–163.
[8] Mohan NS, Kulkarni SM, Ramach A. *J. Mater. Process. Technol.* 2007, 186, 265–271.
[9] Davim JP, Reis P, Antonio CC. *Compos. Sci. Technol.* 2004, 64, 289–297.
[10] Amit Y. Experimental Investigation and Analysis for Bearing Strength Behavior of Composite Laminates. Wichita State University, Master thesis, 2006.
[11] Weimer C, Preller T, Mitschang P, Drechsler K. *Composites, Part A* 2000, 31, 1269–1277.
[12] Massimo D, Antonio L. *Appl. Compos. Mater.* 2009, 16, 297–306.
[13] Karger-Kocsis J, Fejes-Kozma Mech Zs. *Compos. Mater.* 1994, 30, 8–13.
[14] Karger-Kocsis J. *J. Polym. Bull.* 1993, 31, 235–241.
[15] Wang WC, Sheu YM. *Compos. Struct.* 1996, 34, 91–100.
[16] Alaattin A, Ibrahim U. *Compos. Struct.* 2008, 85, 59–63.
[17] Green BG, Wisnom MR, Hallett SR. *Composites, Part A* 2007, 38, 867–878.
[18] Orifici AC, Herszberg I. 27th Congress of International Council of the Aeronautical Sciences, Nice, France, 2010.
[19] Lindhagen J, Berglund LA. *Polym. Compos.* 1997, 18, 40–47.
[20] Mendoza J, Alvaro J, Pipes RB, Koslowski M. *JOM.* 2011, 63, 43–48.
[21] O'Higgins RM, McCarthy MA, McCarthy CT. *Compos. Sci. Technol.* 2008, 68, 2770–2778.
[22] Whitney JM, Nuismer RJ. *J. Compos. Mater.* 1974, 8, 253–265.
[23] Chang FK, Scott R, Springer G. *J. Compos. Struct.* 1984, 18, 290–296.
[24] Kim JK, Kim DS, Takedar N. *J. Comp. Mater.* 1995, 29, 982.